Spring 2020

A Geophysical Survey near Blacktail Creek in the Thompson Park area near Butte, Montana

Guolong Wu

A Geophysical Survey near Blacktail Creek in the Thompson Park area near Butte, Montana

Author: Guolong Wu

Advisor: Dr. Mohamed Khalil

Montana Technological University

Butte, MT 59701

Abstract

Subsurface electrical information can be obtained by electrical and self-potential methods. These geophysical methods, compared to drilling, provide a much cheaper option for investigating the hydrogeological setting. In this project report, we carried out resistivity and self-potential survey along Blacktail Creek in the Thompson Park area near Butte, Montana to understand the hydrogeological setting.

Three geophysical methods have been used: 2D electrical resistivity, 3D electrical resistivity, and self-potential. The least-square inversion resistivity model results showed a general variation of resistivity with depth and delineated the extent of the ground water. The ERT results show three electrical layers, one of them is a water filled alluvial sand layer with a resistivity range of 100-200 Ωm; the layer under the water layer is weathered granite with resistivity range of 200-800 Ωm; resistivity ranges from 800-1100 Ωm indicating granite bedrock. The survey result from the 3D resistivity profile showed relatively high resistivity in the middle of the survey area interpreted as alluvial sand. The layers above and under the middle layer have low resistant, indicating water flow and water reserves. The self-potential result indicates there is a probable downward flow ground water in the area adjacent to the stream. This downward flow was interpreted as the creek is charging ground water. Environmental managers can refer to this knowledge to have a better sense of locations with high potential to hold ground water so beaver mimicry sites can be better located to leverage water storage.

Table of Contents

1. Introduction

Beavers are native animals to Thompson Park. They work at night and build dams that form a pond in order to protect themselves from predators. Beaver dams slow down water flow, expanding the contact area between water and rock, allowing more water to be held upstream because water is spread out over a greater area. When this happens, there is a better balance between peak water flow in summer and diminished flow in winter. These beaver dams act as buffers and are the critical structures for the whole ecosystem, making beaver an essential species to the environment with limited water flow. In recent years, beaver populations have decreased due to trapping. As a result, fewer beaver dams are being built, depriving the watershed of their benefits. Beaver mimicry structures can be made and installed to fill this void. Based on the geological and hydrogeological setting, knowledge as to locations with high potential to reserve water is necessary for making effective decisions on the position of such replacement dams. In this project, the resistivity method and the self- potential method are used to investigate the geological and hydrogeological setting along Blacktail Creek in Thompson Park so that environmental managers have requisite information for decision making.

1.1 Site description

Our investigation was carried out on a floodplain formed by Blacktail Creek. The width of the floodplain is about 100 meters, and it stretches to about 1000 m long. The location of investigation is approximately 30 km south of Butte, Montana, which is shown in Figure 1.

Based on the Köppen climate classification (Rubel & Kottek, 2011), the climate for the area of study is semi-arid with precipitation that is below potential evapotranspiration, but not as low as a desert climate. The yearly average temperature of the region is from -3.6 °C to 11.9 °C.

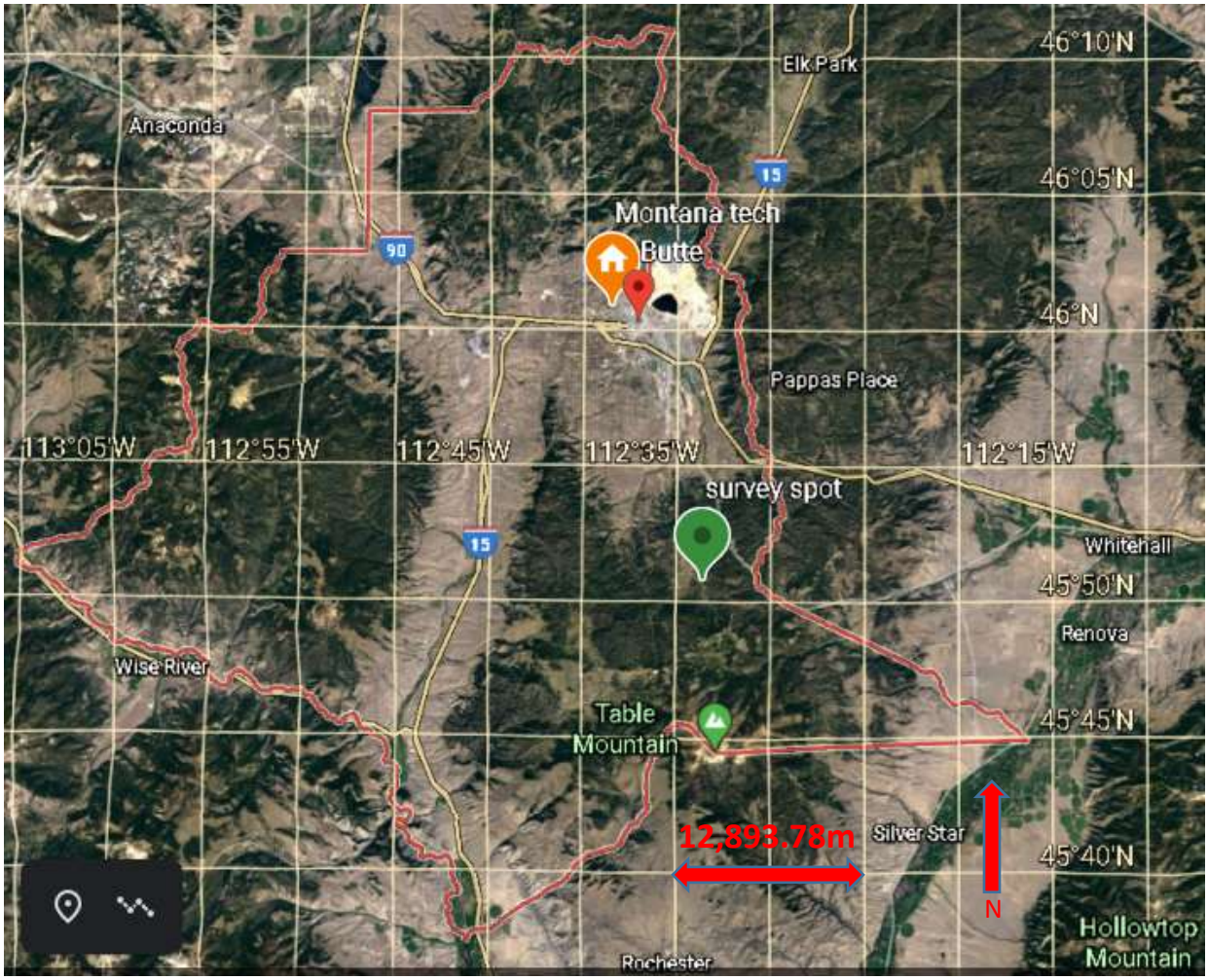

Figure 1. Overview of study location. The line in red is Silver Bow County. The green spot is where the study was carried out. The spot in copper denotes the Montana Tech.

1.2Geological setting

1.2.1 Regional setting

The Climax Gulch pluton is underlain by granite and is just to the south of the Boulder Batholith circled in blue in Figure 2. The area of focus is in the Climax Gulch Pluton shown in Figure 3 by yellow. The following tectonic areas and characteristics have an impact on the Boulder Batholith, including:

1. Boulder Batholith: a big granite mass dated from the Cretaceous period.

2. Lewis and Clark line: it stretches over 500 miles from the middle of Montana to northeastern Washington and runs north of Silver Bow County. Mesoproterozoic folds and faults are

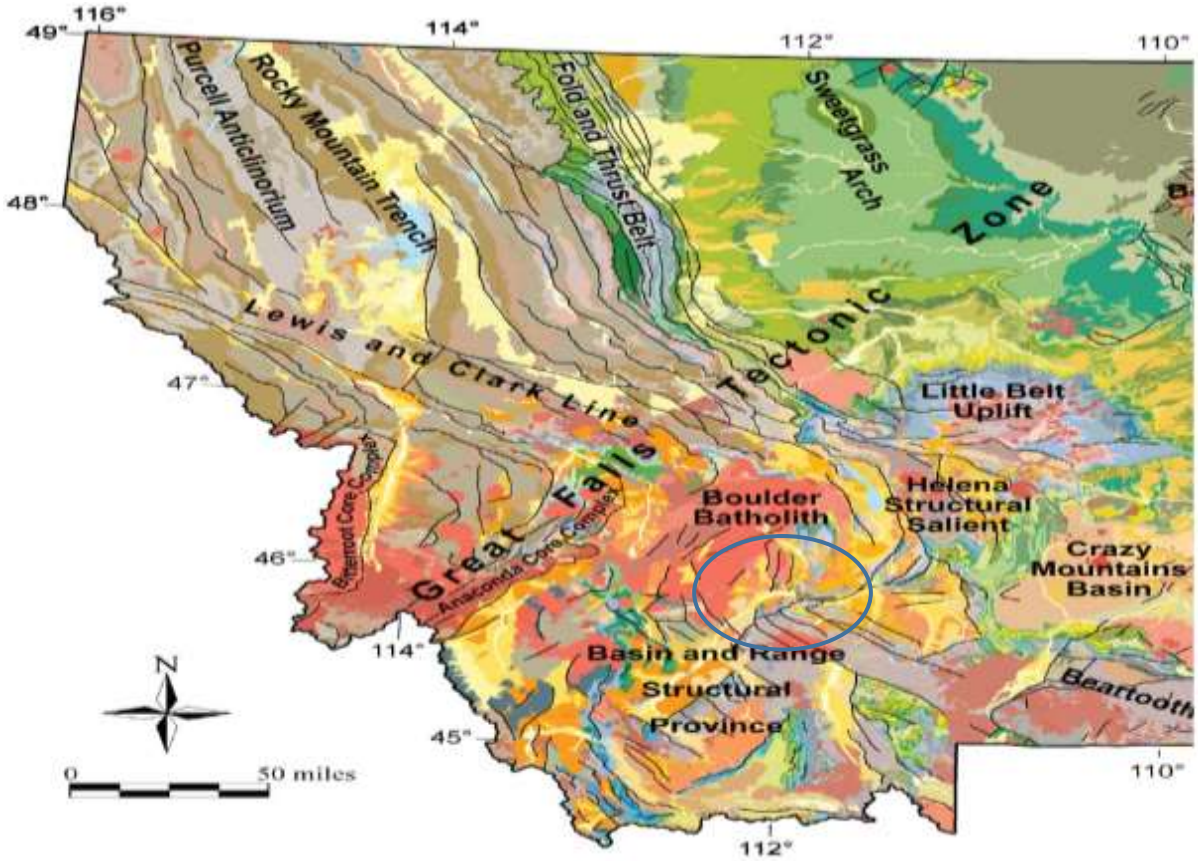

Figure 2. Tectonic zones of western Montana (McDnald, 2009). The area circled in blue denotes the location of the geophysical survey.

found in the Lewis and Clark line (Harrison, 1974; Goode, 1979; Winston, 1986; Wallace, 1990; Sears, 2004)

3. Helena Salient: this is a bulge of Front Range-style folding and thrust faulting. "The southern edge of the Helena Salient is the South Montana Transverse Zone or Perry Line which crosses Silver Bow County runs through the Highland Mountains." (McMannis, 1963)

4. The Great Falls Tectonic Zone: this is to the west of the Boulder Batholith and is right on the top of the Paleoproterozoic layer, which features in the northeast-trending faults. It is distinguished by igneous rocks.

5. The Basin and Range Province: this area is within and around the Boulder Batholith and is part of the Rocky Mountains which stretches more than 2982 miles from British Columbia all the way to New Mexico (Cheney, 1994).

1.2.2 Boulder Batholith and Climax Gulch Pluton

The Boulder batholith shown in Figure 3 (a) is a body of granite rock, stretching from the Highland Mountains to the vicinity of Helena. It is about fifty miles from north to south, and twenty-four miles' in width. The batholith is made from the intrusion of multiple plutons, the largest of which are the Butte Granite and the Climax Gulch pluton. U-Pb zircon geochronological investigations have shown that all intrusions of the Boulder batholith are from the Cretaceous era. The estimated age for the Boulder batholith plutons is from 77.6 to 73.7 Ma, and the Butte Granite is from 76.5 to 74.5 Ma. Early K-Ar age data show that the Climax Gulch pluton, which is one of the Boulder batholith intrusions, might be as young as ≈ 68 Ma (Bray, 2009). The area circled in blue in Figure 3 (a) contains the survey location, which is part of Boulder batholith. Figure 3 (b) is the legend for Figure 3 (a).

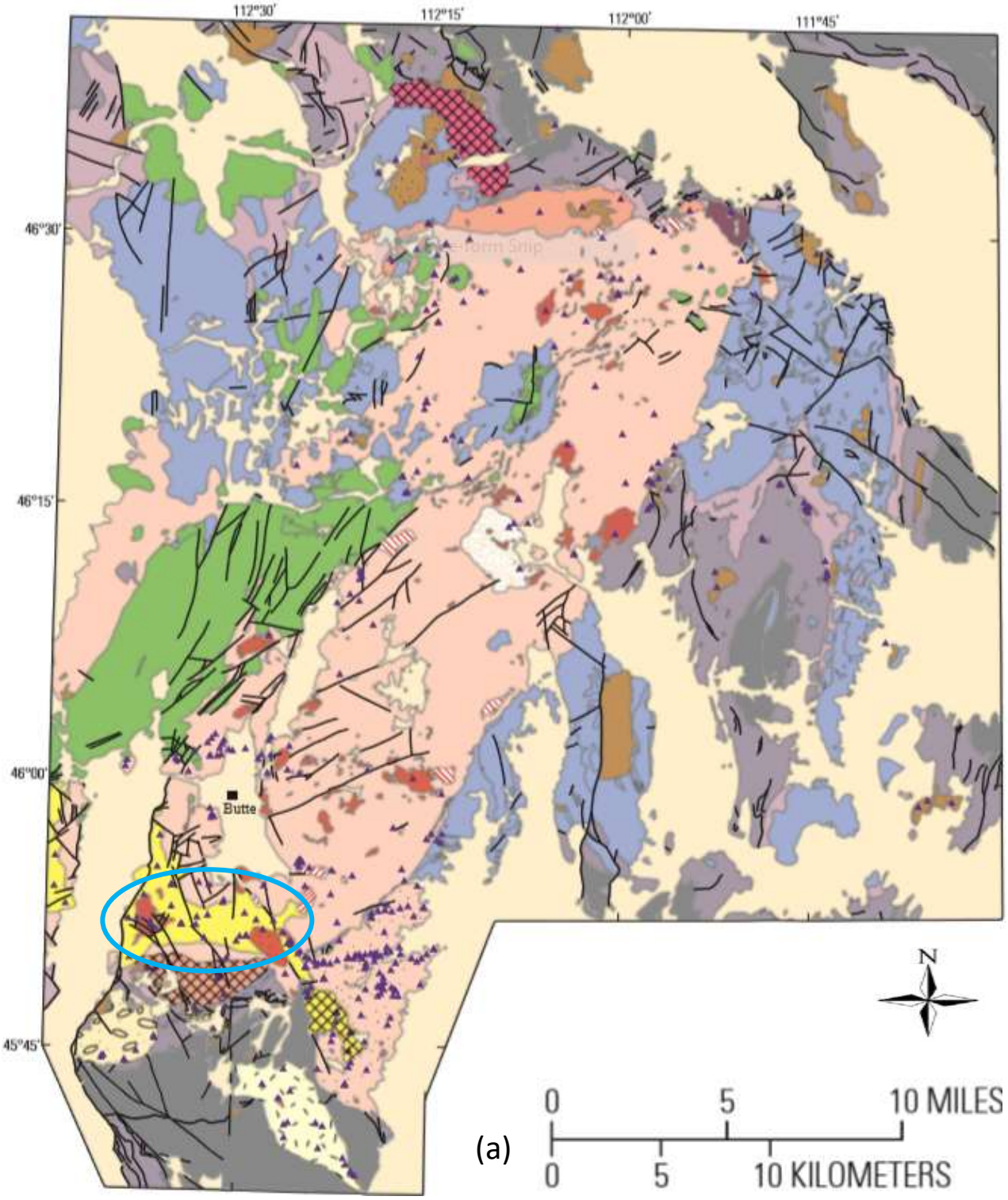
112°30'
112°15'
112°00'
111°45'
46°30'
46°15'
46°00'
45°45'
Butte
N
0
5
10 MILES
0
5
10 KILOMETERS

(a)

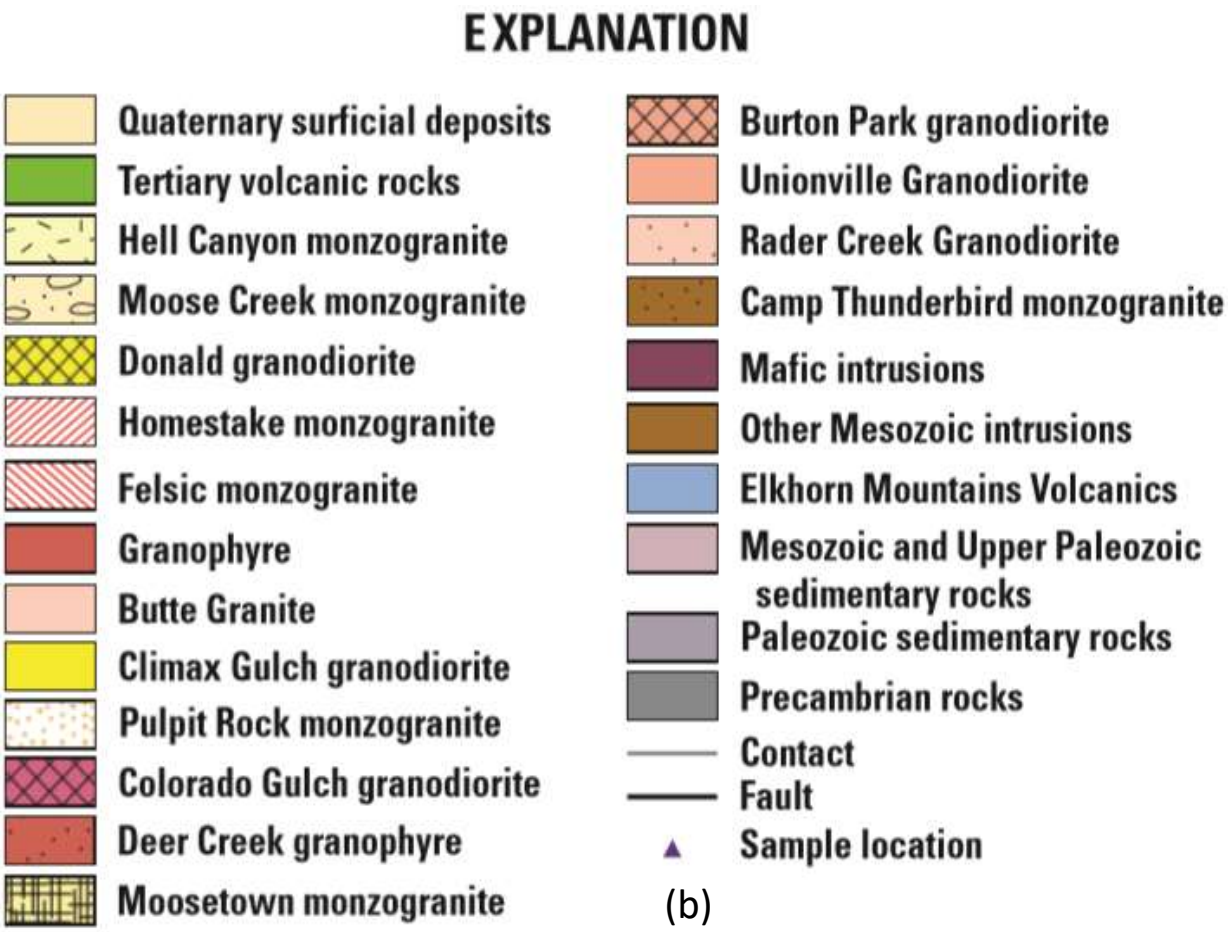

Figure 3 Panel (a) is Geology for Boulder Batholith map (Edward A. du Bray, 2012), the area circled in blue is the study area. Panel (b) is an explanation for panel (a).

2. Theory

2.1 GPS Survey

Survey station locations were obtained with an Emlid Reach RS GPS system with two receivers. One receiver is stationary and is called a base station. The second is mobile and is called the rover.

2.2 Electrical Resistivity Tomography (ERT)

Even though groundwater cannot be seen on the Earth's surface, various geophysical methods can be applied to get underground information. Among geophysical methods, the electrical resistivity method is the most useful and cost-effective technique for groundwater studies. The electrical resistivity contrasts that exist across interfaces of lithologic units in the subsurface are used to delineate discrete geoelectric layers and detect aquiferous or non-aquiferous layers (Aweto, 2013). The resistivity method uses four-electrodes, where two current electrodes inject electric current into the soil and two potential electrodes measure the potential difference. Based on Ohm's law, the apparent electrical resistivity in the midpoint of the array can be calculated using a geometric factor. Many arrangements (arrays) are available to carry out a resistivity survey, such as dipole- dipole, Schlumberger, pole-pole and Wenner array (China Patent No. CN201621237537, 2017). In this project, we used the Wenner alpha array shown in Figure 4, because of its high vertical resistivity resolution and high signal-to-noise ratio. The four-electrodes system is moved along the profile to collect data for the first data line, and then the electrode spacing is increased to get resistivity values of deeper parts of the profile (Keller, 1966).

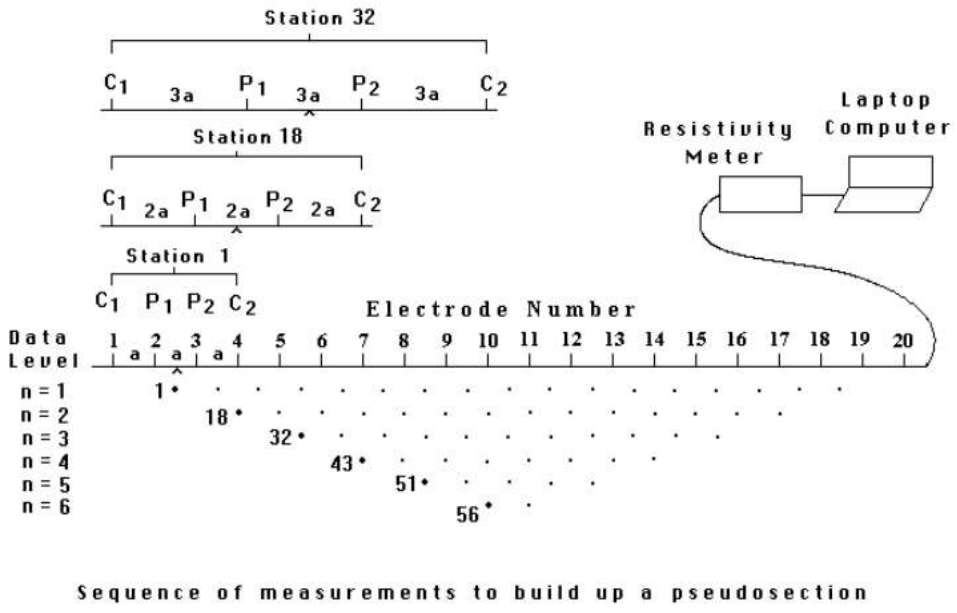

Figure 4. The arrangement of electrodes for a 2-D electrical survey and the sequence of measurements used to build up a pseudosection (Loke, 2000).

2.3 Self-potential (SP)

The self-potential (SP) method measures the natural potentials caused by electrochemical or electrokinatic processes in the subsurface. No current is required in this method, making it the cheapest and simplest option. The equipment required to carry out the SP survey consists of two non-polarizing electrodes and a multimeter, along with the connecting wire. The potential gradient method and the total field method can both be applied to collect data. In the potential gradient method shown in Figure 5 (a), two electrodes at fixed intervals are used to measure a potential difference. The potential difference is then divided by the fixed electrode space to calculate the potential gradient. The point measured is in the middle between the two electrodes. After that, the two electrodes are leap-frogged along a traverse. The potential shown in Figure 5(a) is then recorded. The advantage of this method is the short length of connecting wire; however, a disadvantage is that there could be a cumulative error. In the total field method, shown in Figure 5 (b), one electrode is fixed at a base station outside the area of exploration, and

a mobile electrode is moved along the profile. In contrast to the potential gradient method, this method needs a long wire, but it has a smaller cumulative error and avoids any confusion in polarity. Self-potential has been used to detect massive ore bodies and groundwater, as well as for geothermal exploration (Oskay, 1978). In this project, the total field method was used.

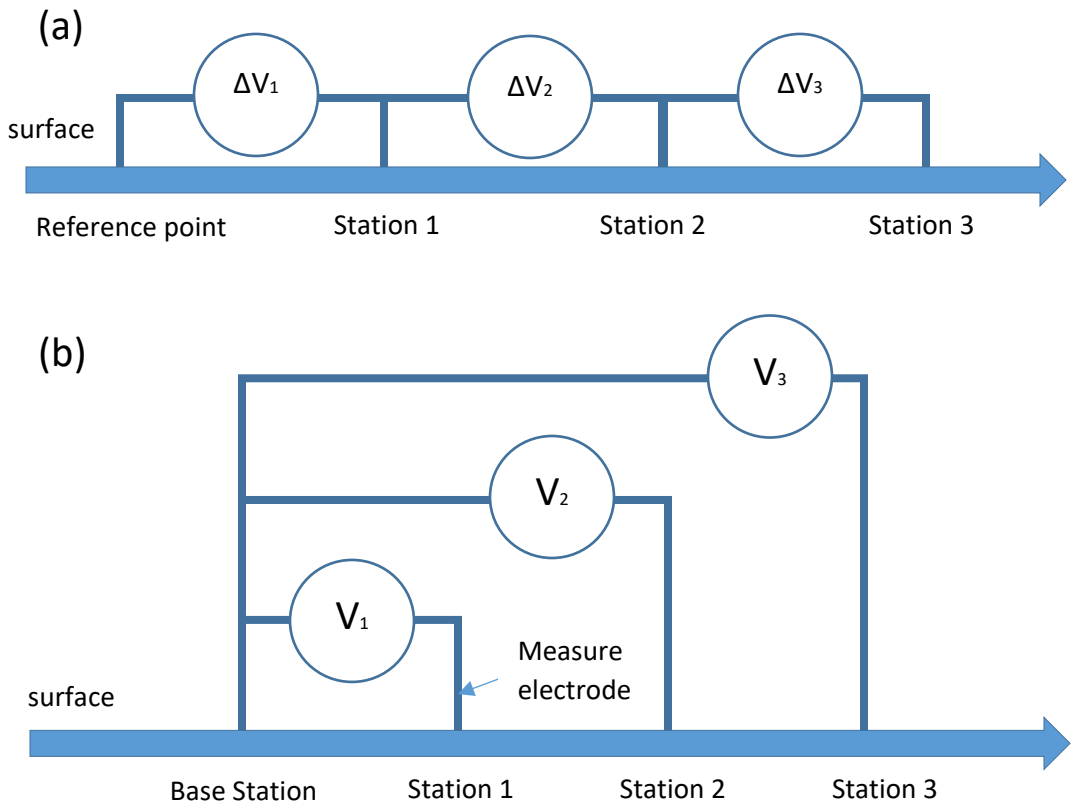

Figure 5. Two methods for setting up electrodes for self-potential measurement. The gradient method shown in panel (a) uses two electrodes "leapfrog" to cover the area being profiled, the measurement electrode of total field method shown in panel (b) starts at station 1, then moves to station 2 until the profile is finished.

3. Survey

From May 14th through May 16th, field data was collected including four 2-D surveys, one 3-D survey, and a gridded self-potential (SP) survey.

3.1 2-D resistivity

In our 2D resistivity survey, four lines were set up through the area of study, Lines 1 and 2 were perpendicular to the creek, while Lines 3 and 4 were parallel to the creek, as shown in Figure 6. Each survey line was 200 m in length and included 21 electrodes with 10 m inter-electrode space. This space was increased by 10 m increments up to 60 m with the same 200 m overall length. Each line has 63 data points collected by SYSCAL-R2 resistivity meter with a 12 V battery and a 250 W DC-DC converter. The yellow rectangle in Figure 6 shows the position of our 3D resistivity and self-potential survey. The expansion of the survey is shown in Figure 7.

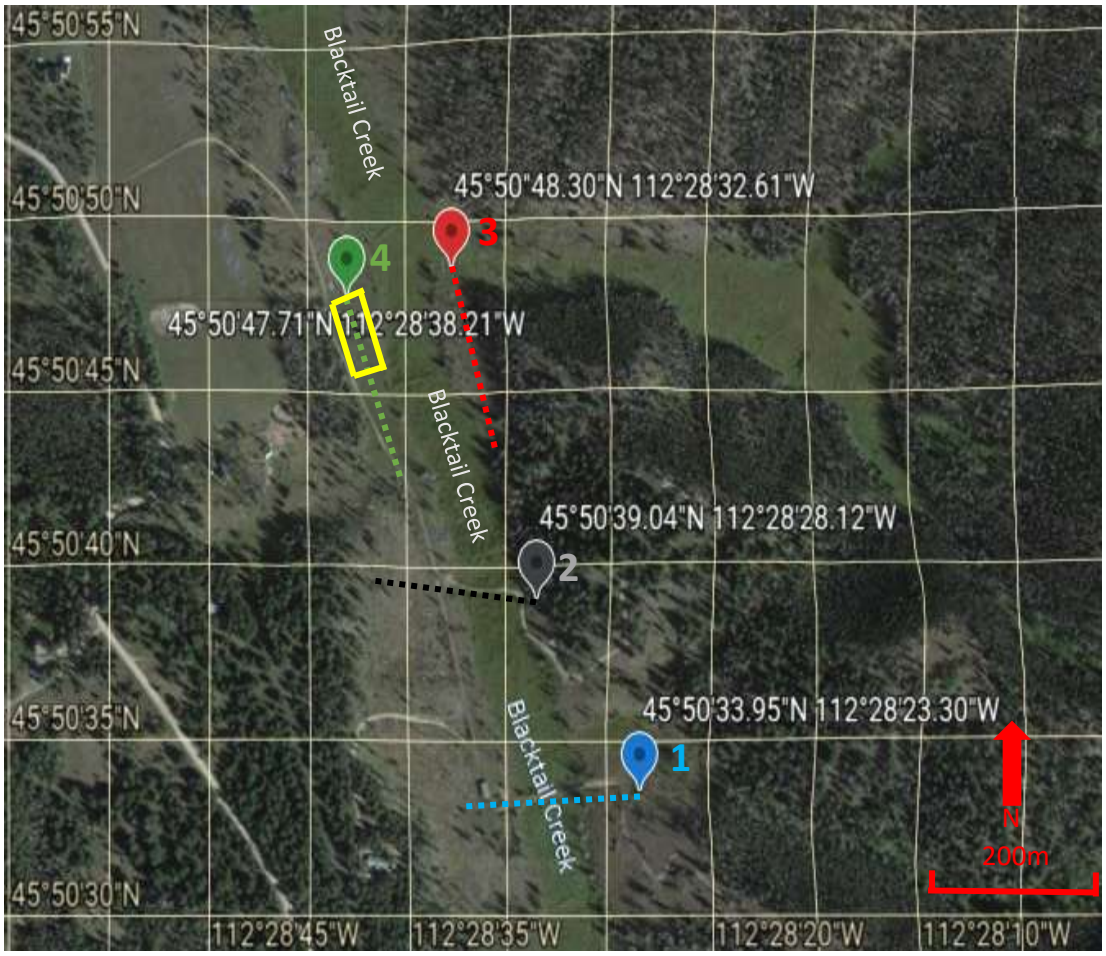

Figure 6. Location for each profile. The blue, black, red, green lines stand for the location of 2D survey lines. The yellow lines in the figure show the location of the 3D survey.

3.2 3-D resistivity

We used the Wenner 3-D array in a grid composed of five 100 m profile lines with 21 stations and 5 m intervals to cover an area of 100 m by 20 m shown in Figure 7. Each yellow survey line on Figure 7 produced 63 data collection points. The 3D data was collected by a SYSCALR2 resistivity meter.

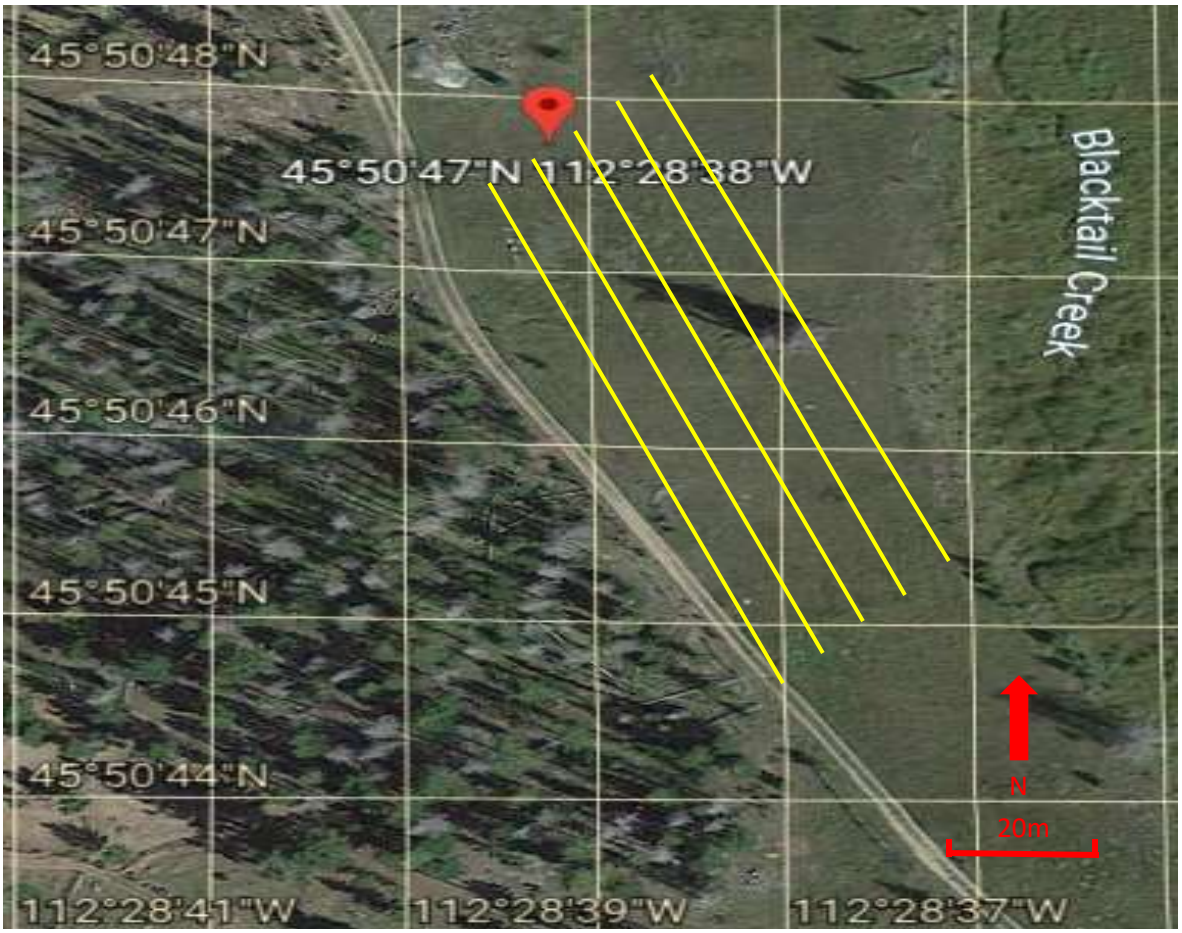

Figure 7. 3D resistivity and self-potential layout indicated by yellow lines

3.3 Self-potential

The self-potential survey was carried out in the same grid pattern of 100 m by 20 m as the 3D resistivity survey shown in Figure 7. The total field method was used in this survey. A non-polarizing electrode shown in Figure 8 remained at the base station while another one successively moved along the width of the grid pattern, then the profile was moved 5 m interval along the length, and the repeated pattern continued until all of the grid was covered. Overall 65 data points except the base point were collected for this survey.

Figure 8. The saturated lead chloride non-polarizing electrode that we used.

4. Data Processing

To get an underground resistivity profile, the resistivity data were obtained by DC resistivity meter Syscal R2 manufactured by IRIS instruments and self-potential data were obtained by the multimeter.

4.1 2-D resistivity

The following steps were used to process the data with the RES2DINV. First, the field data were put into a txt file in the required format specifically for Wenner array (Bhd, 2019). To get a good model, error analysis was applied to guarantee quality. Then 5 iterations of robust least-square inversion were performed.

4.1.1 Error analysis.

a) Pre-inversion analysis. As a general rule, before carrying out the inversion of a data set, we take a look at the data as a pseudosection plot. Bad data points show up with unusually low or high values. In profile form, they stand out from the rest and can be easily removed manually from the data set by removing the point in the pseudosection plot.
b) Post-inversion analysis. The preliminary inversion is applied to the data. RMS error analysis was carried out on the data so that the data with large RMS values contaminated by noise could be removed.

4.1.2 Further inversion

Following the RMS error analysis, further inversion was again applied to the data. If the overall RMS error was over 5%, RMS error analysis was continually applied until the result was less than 5%.

4.2 3-D resistivity layers and block model

These data were processed to get the inversion result. The results were then displayed using Surfer8. Based on the geology and tectonics of the area, we had hypothesized that the investigated site would consist of discrete subsurface structures with sharp boundaries between different bodies. A robust model inversion technique was more suitable for this type of case. However, if the subsurface bodies have gradational boundaries (e.g. bedrock with a thick transitional weathered layer), the conventional smoothness-constrained inversion method might yield more realistic models (Neyamadpour, 2009).

4.3 Self-potential

After the survey, a drift correction was applied to eliminate the temperature impact on data. First, we calculated the time difference relative to base station denoted by A, and then obtained the difference denoted as B by subtracting first base reading from final base reading. The drift correction was the product of A and B. The drift corrected reading was then acquired by subtracting the drift correction from each original reading. A contour map was created to show the distribution of electrical potential at the ground surface relative to the potential at the base station for each site.

5. Discussion and Results

5.1 2-D resistivity

The RES2DINV software produced a resistivity profile using the data collected by four 2-D survey lines.

The profiles in Lines 1 and 2 contain distinct topographic variations, while Lines 3 and 4 were flat enough to ignore the minor topographic variation. In these results, the color scales are the same in all four images; blue stands for the low resistivity range of 100-200 Ωm, and indicates ground water in porous alluvial sand; purple and red indicate a high resistivity range of 800-1100 Ωm, which is interpreted as granite bedrock. The layer between the water layer and granite bedrock layer is interpreted as weathered granite with resistivity range from 200 Ωm to 800 Ωm. In the profile of Line 1 shown in Figure 9, the low resistivity part is in the middle. One possible fault is around 100 m in the profile of Line 1 where there is a sharp boundary between water flow and granite bedrock. In the profile of Line 2 in Figure 10, the largest portion of low resistivity was located on the left side of the profile between 40 m and 90 m.

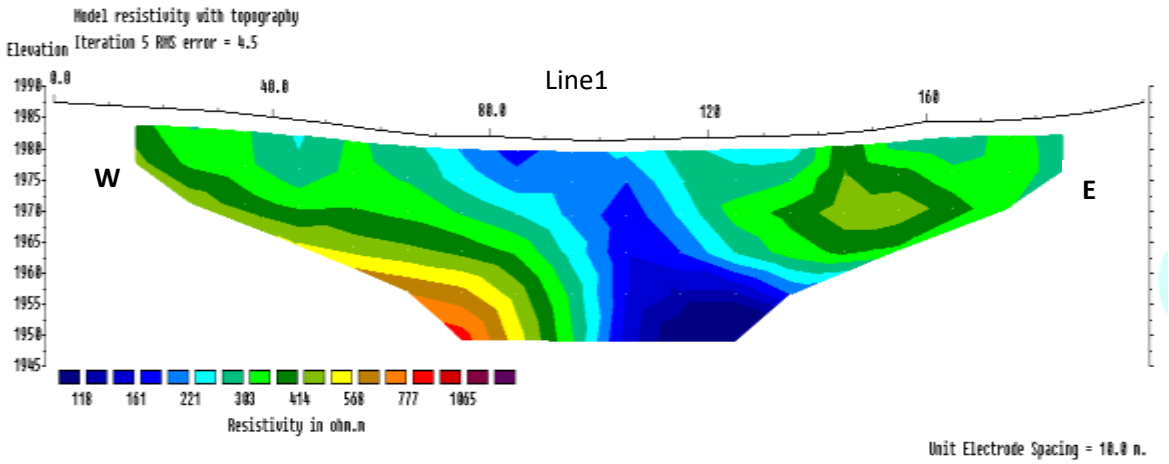

Figure9. Inversion result of Line 1.

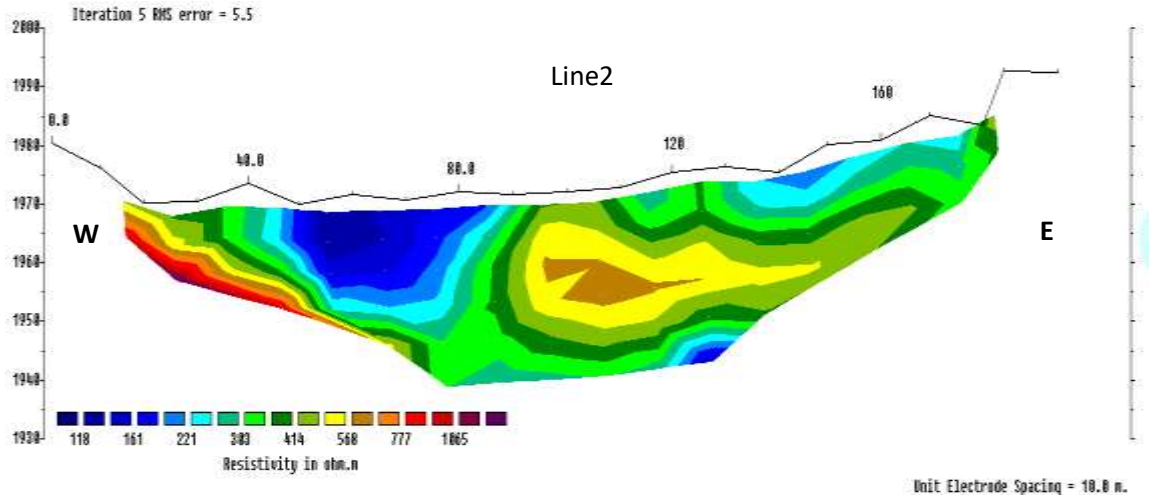

Figure 10. Inversion result of Line 2.

In the profile of Line 3 in Figure 11, the low resistivity area was near the north end of the survey, with overall resistivity increasing toward the south end of the survey.

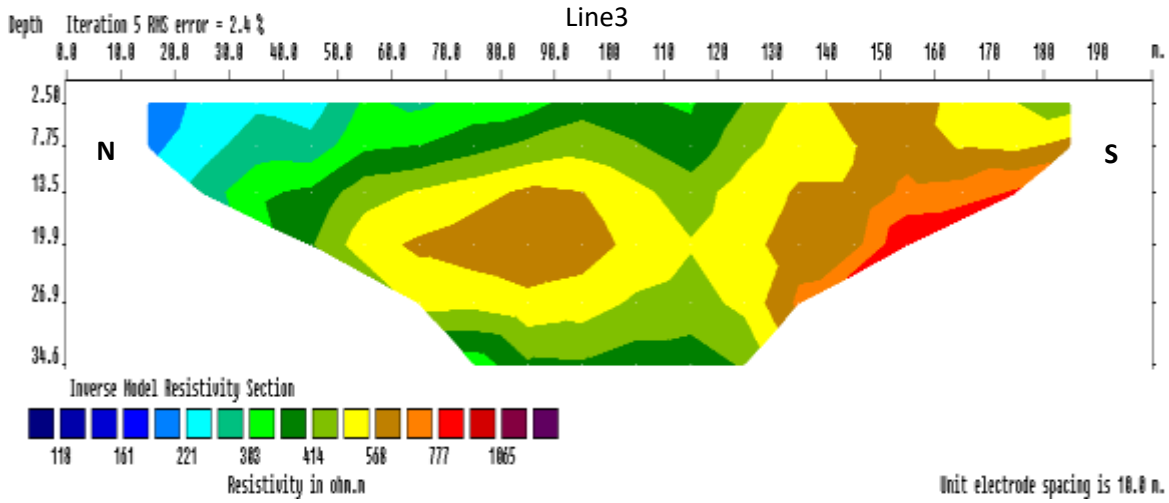

Figure11. Inversion result of Line 3.

In the profile of Line 4 in Figure 12, the point circled in blue was removed. Before removal, the error was greater than 20% for the profile on Figure 13. After removal, the error is less than 2% shown in Figure 14. Most of the area in the profile of Line 4(b) was saturated with ground water, overall resistivity increasing from the north end to the south end of the survey.

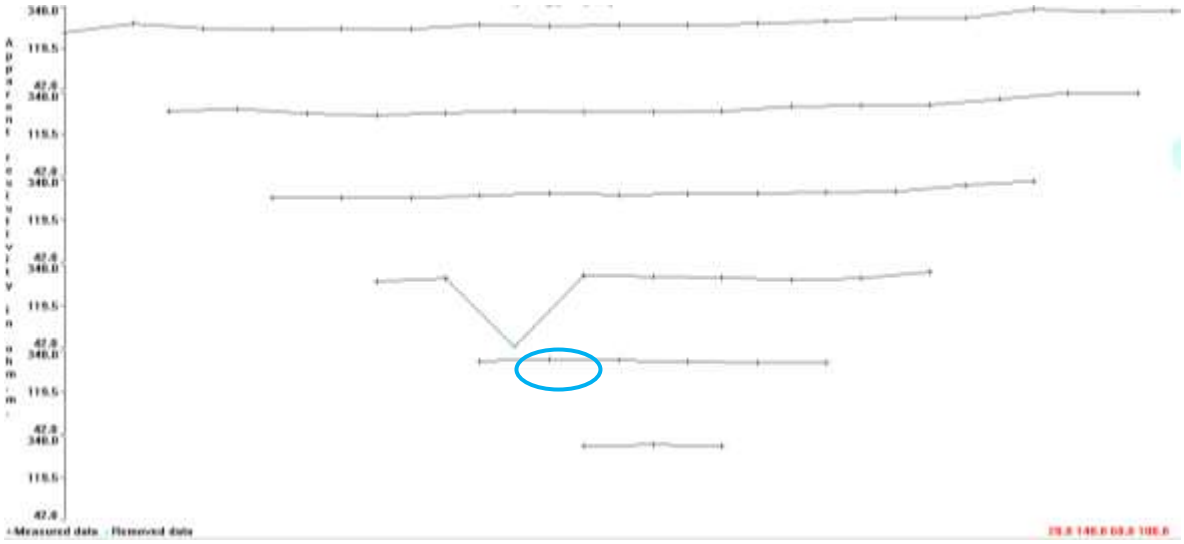

Figure 12. The process for eliminating a bad data point circled in blues.

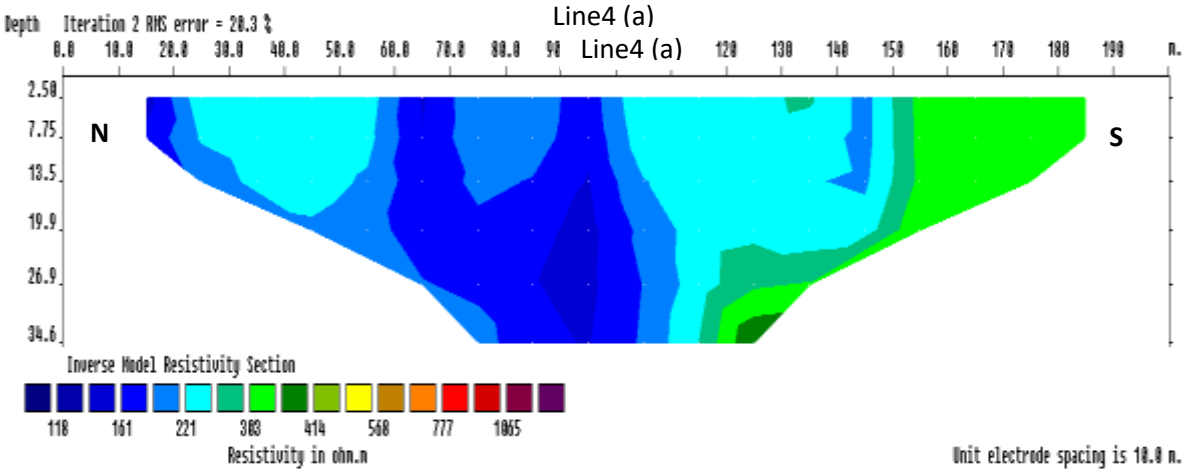

Figure 13. Reversion result of Line 4 prior to bad data point elimination.

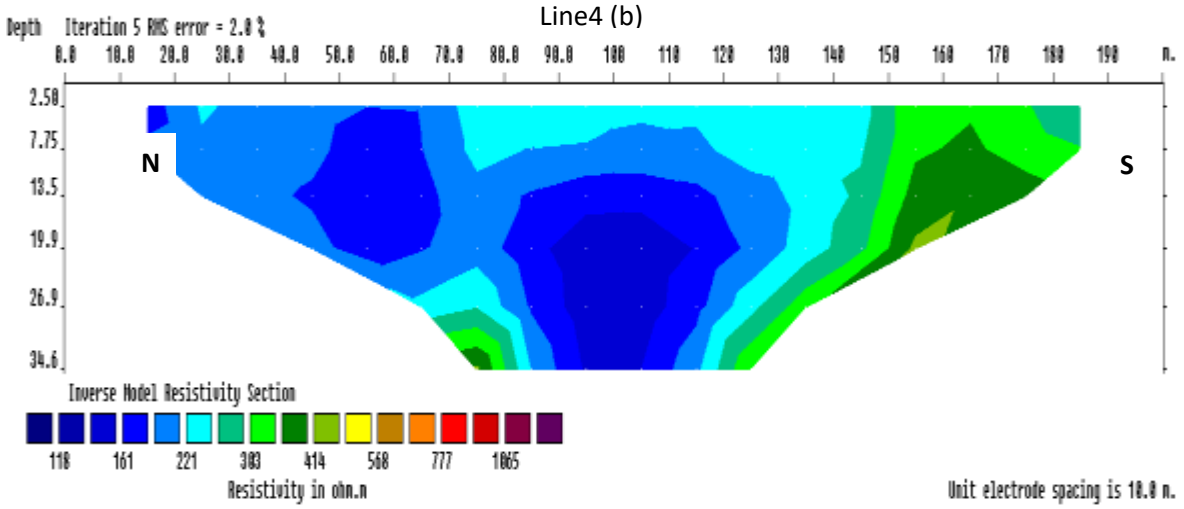

Figure14. Inversion result for Line 4 after removing the bad data point.

5.2 3-D resistivity

First, RES3DINV software was used to produce 5 maps for different depths shown in Figure 15. These inversion files were then saved as XYZ file. After that, Surfer 8 software was used to produce the profile for each layer shown in Figure 16. The profiles at each depth were cut based on the 2D inversion result shown in Figure 16.

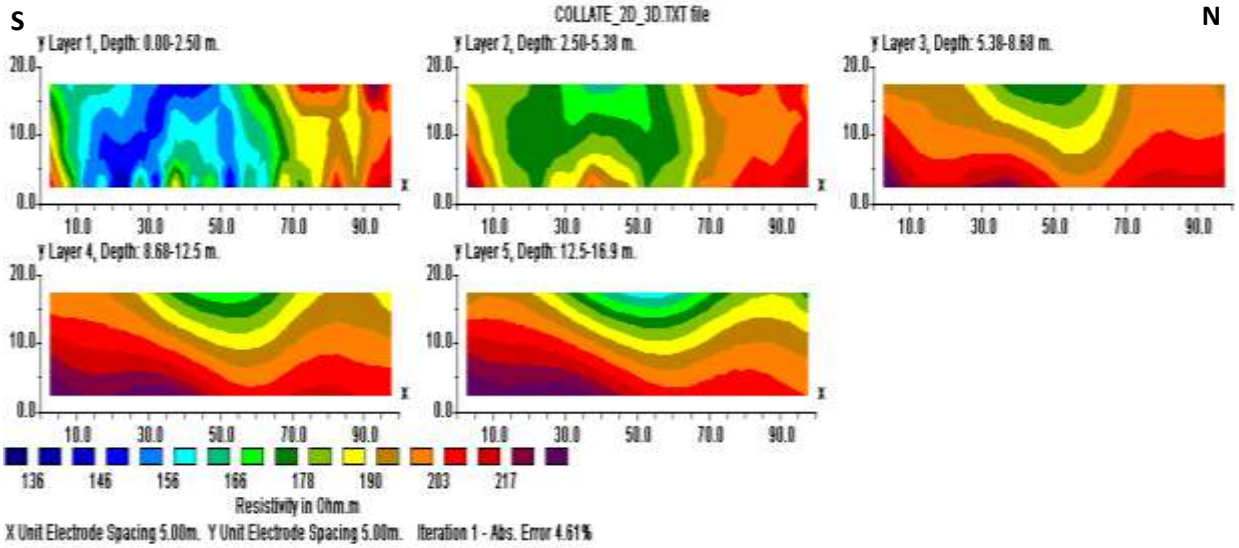

Figure 15. The 3D inversion result using RES3D software.

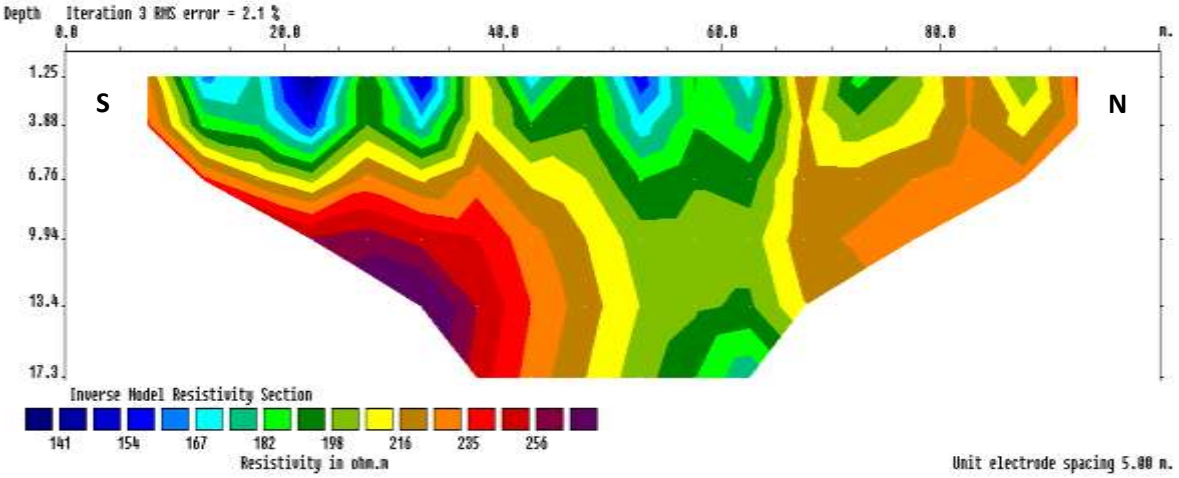

Figure 16. One of the 2D inversion profiles used to cut the pictures at each depth.

In the end, all profiles were combined in a 3D model shown in Figure 17, a big conductive zone appears at a depth ranging from surface to around 4 m. Resistivity is relatively high at depths from 5m to 10m indicating alluvial sand, however, the resistivity is very low at depths around 11m. The portion circled in purple is interpreted to be saturated with water.

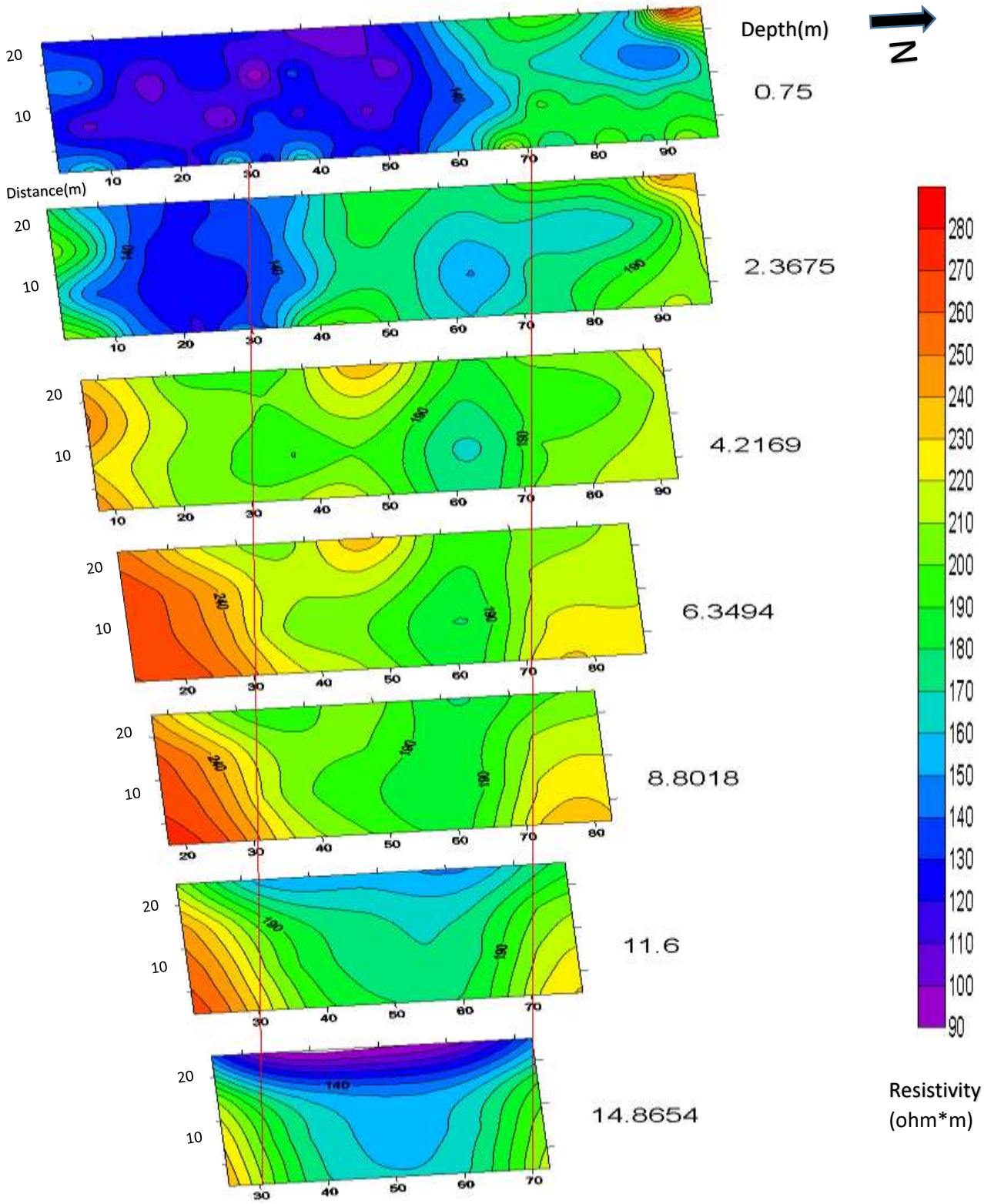

Figure17. The 3D profile at different layers.

5.3 Self Potential

The flow of ground water generates a detectable polarization of electrical charge in the ground, called the streaming potential. It can be observed at the ground surface through passive self-potential measurements of the electrical potential with nonpolarizable electrodes. “The first-order linear least-squares separation was applied to the observed field data shown in Figure 18(a) to separate the residual and regional effect of streaming potentials. The residual data shown in Figure 18(c) reflects the shallow media where surface water is the dominant source of self-potential measurements, and the regional data shown in Figure 18(b) reflects the groundwater system, mapping the regional groundwater flow direction.” (Prudhomme, et al., 2019)

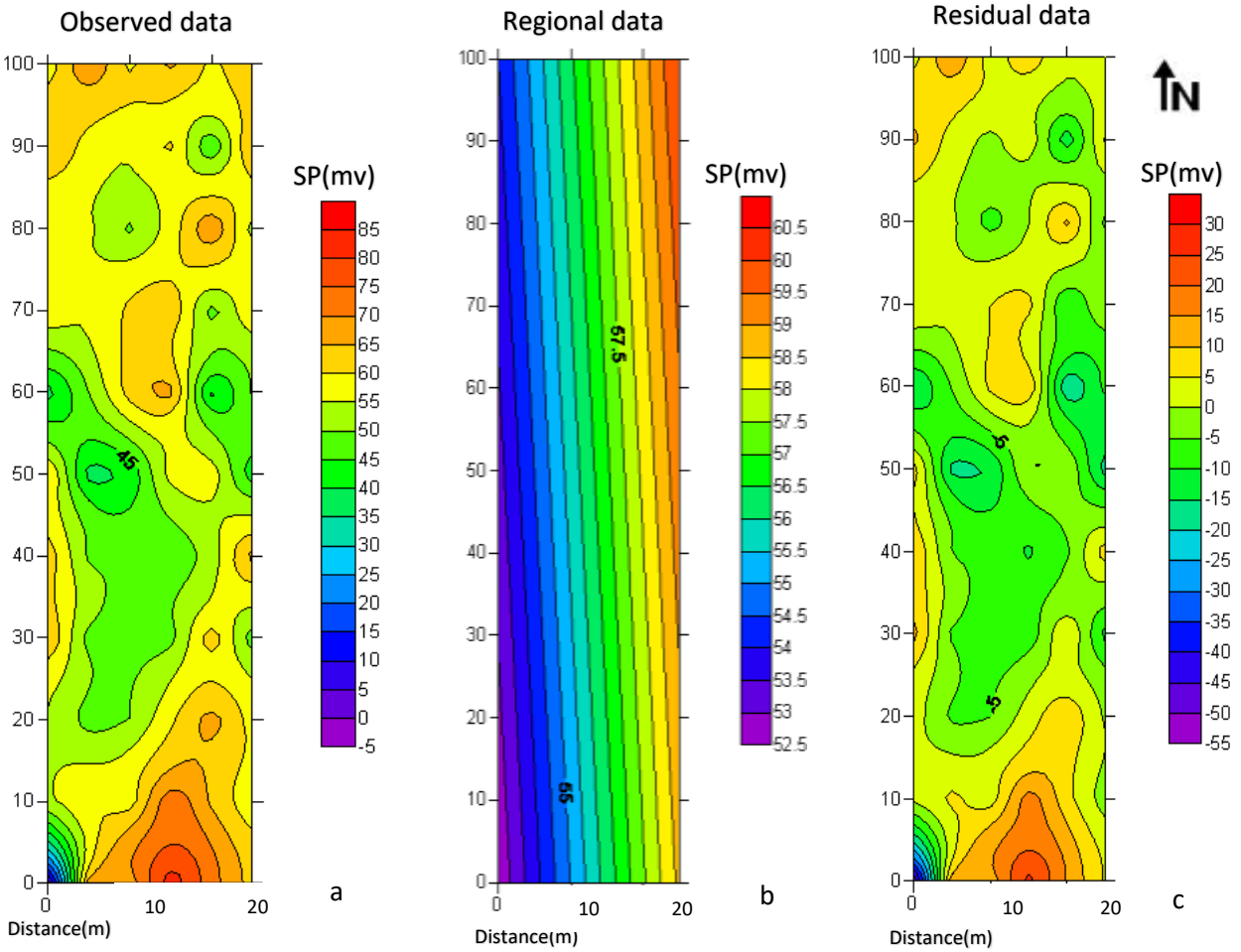

Figure 18. Panel a shows raw self-potential data, Panel c shows corrected self-potential after removing the regional data shown in panel b.

In Figure 19, the SP map at the top is compared with vertical resistivity cross sections. The SP map shows relatively low potential in the middle of the survey area indicated by green. In the cross sections, the high resistivity areas are located at the edge of the survey area, while low resistivity areas are in the middle and match the negative SP zone, which indicates a probable downward seepage of surface water to groundwater (Reynolds, 2011).

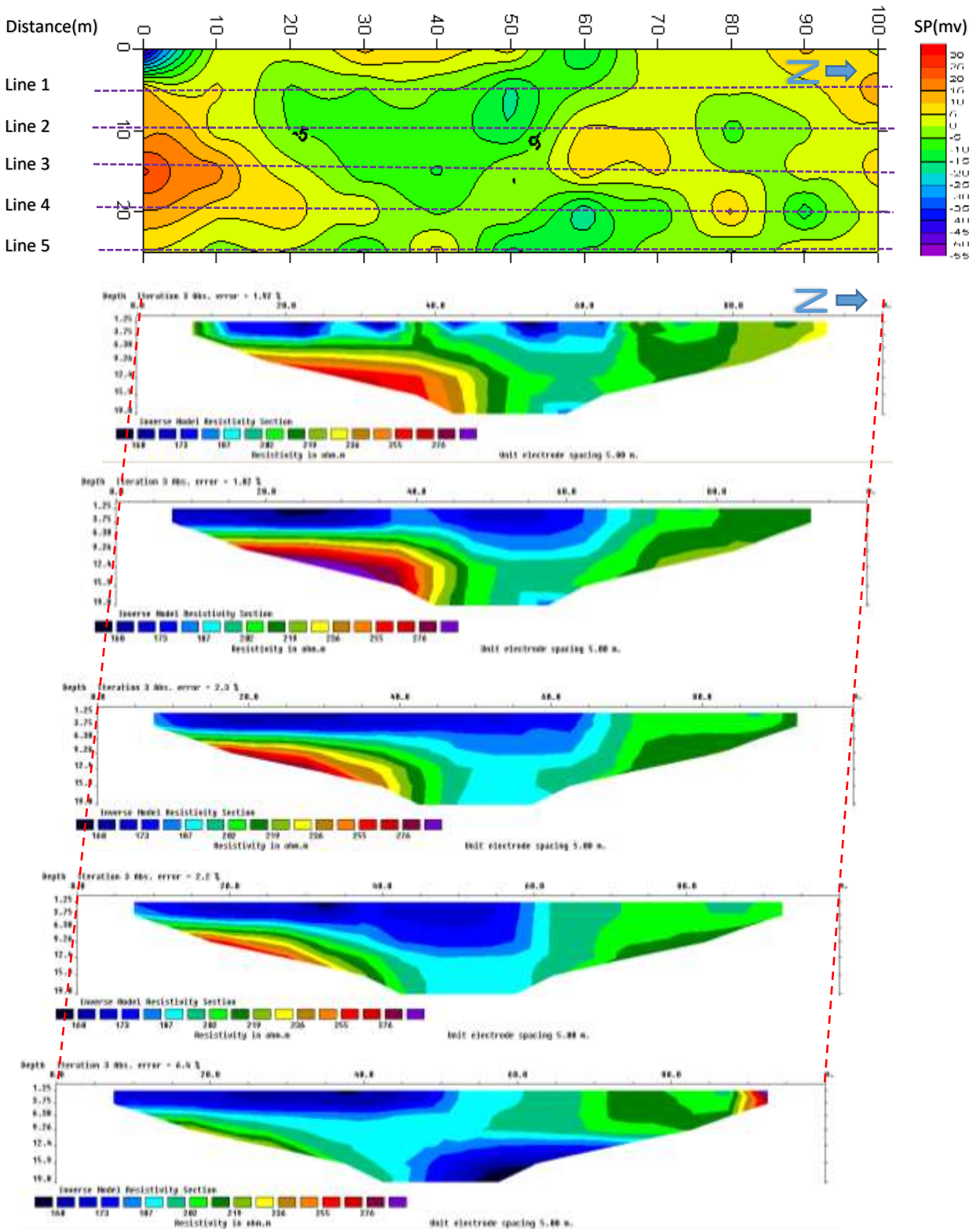

Figure 19. Comparison between SP map and resistivity cross sections.

6. Conclusions

To define the hydrogeological system, 2D and 3D resistivity, as well as self-potential were used to get subsurface information.

From roughly 70 m to 110 m in the profile of Line 1, and from 45 m to 90 m in the profile of Line 2, the low resistivity areas, in the profiles of the two lines crossing the creek, can be interpreted as creek water flowing through the valley. Other areas appearing in yellow or red are granite bedrocks around the creek. One possible fault is in the middle of the profile in Line 1 shown by a sharp contact between what was interpreted as water filled alluvial sand and granite bedrock.

Profiles of Line 3 and Line 4, which are parallel to the creek, show low resistivity at the north end of the survey, and an overall increase in resistivity moving towards the south end of the survey. Overall resistivity in Line 3, however, is higher than Line 4. Granite bedrock and alluvial sand account for most of the profile in Line 3, while the profile in Line 4 consists of mostly water filled alluvial sand and weathered granite. There are two areas saturated with water from approximately 40 m to 70 m along the profile on the surface and from 80 m to 120 m at the depth of 10 m to36 m.

The 3D resistivity model shows low resistivity areas on the surface, and the negative value in the SP profile indicates that the water flow goes downward through alluvial sand. At a depth of 11 m, another low resistivity area shows up and the area is interpreted to be saturated with water, probably from the surface due to the negative SP value on the surface, meaning that creek is

being charged by groundwater. This geological introduction will help environmental managers decide where to construct mimicry beaver dams.

7. References

Aweto, K. E. (2013). Resistivity method in hydro-geophysical investigation for groundwater in Aghalokpe, Western Niger Delta. *Global Journal of Geological Science, 11.1*, 47-55.

Bhd, G. S. (2019). *Rapid 2-D Resistivity & IP inversion.*

Bray, E. A. (2009). *Geochemical database for the Boulder batholith and its satellitic plutons, southwest Montana: U.S. Geological Survey Digital Data Series 454.* Geological Survey (U.S.).

Cheney, E. S. (1994). Tectonics of the Yellowstone hotspot wake in southwestern Montana: Comment and Reply . *Geology, 22(2)*, 185–187.

Edward A. du Bray, J. N. (2012). *Synthesis of Petrographic, Geochemical, and Isotopic Data for the Boulder Batholith, Southwest Montana.* Geological Survey (U.S.).

Goode, H. D. (1979). *Basin and Range Symposium and Great Basin Field Conference.* Denver: Rocky Mountain Association of Geologists.

Harrison, J. G. (1974). *Tectonic features of the Precambrian Belt basin and their influence on post-Belt structures.* Geological Survey.

Keller, G. V. (1966). Electrical methods in geophysical prospecting. In G. V. Keller, *Electrical methods in geophysical prospecting.* Oxford, New York, Pergamon Press.

Loke, D. (2000). *Electrical imaging surveys for environmental and engineering studies,A practical guide to 2-D and 3-D surveys.*

McDnald, C. G. (2009). *Geologic Map and Geohazard Assessment of Silver Bow County, Montana.* Butte, Mont: Montana Bureau of Mines and Geology.

McMannis, W. (1963). LaHood Formation: A coarse fa-cies of the Belt Series in southwestern Montana. *Bulletin of the Geological Society of America, 74(4)*, 407-36.

Neyamadpour, S. T. (2009). An application of three-dimentional electrical resistivity imaging for the detection of an underground waste-water system.

Oskay, M. (1978). *Self-potential profiling : laboratory and field studies of the thermoelectric effect on inhomogeneous porous media.* ProQuest Dissertations and Theses.

Prudhomme, K. D., Khalil, M. A., Shaw, G. D., Speece, M. A., Zodrow, K. R., & Malloy, T. M. (2019). Integrated geophysical methods to characterize urban subsidence in Butte, Montana, U.S.A. *Journal of Applied Geophysics, 164*, 87-105.

Reynolds. (2011). An Introduction to Applied and Environmental Geophysics. *Preview , 2011(155)*, 33-40.

Rubel, F., & Kottek, M. R. (2011). Comments on: “The thermal zones of the Earth” by Wladimir Köppen. *Meteorologische Zeitschrift, 20(3)*, 361-365.

Sears, J. W. (2004). Lewis and Clark line and the rotational origin of the Alberta and Helena salients, North American Cordillera . In A. J. Sussman, *Orogenic curvature: Integrating paleomagnetic and structural analyses* (Vol. 383). Geological Society of America.

Wallace, C. L. (1990). Faults of the central part of the Lewis and Clark line and fragmentation of the Late Cretaceous foreland basin in west-central Montana. *Geological Society of America Bulletin, 102(8)*, 1021-1037.

Winston, D. (1986). Stratigraphic correlation and nomenclature of the Middle Proterozoic Belt Supergroup, Montana, Idaho, and Washington, in Roberts, S. M., ed., Belt Supergroup. *Montana Bureau Mines and Geology*.

Yongjun, Y., Xiaoxiao, Q., Fangnan, W., Bing, S., Yong, L., Liang, W., . . . Kangping, T. (2017). *China Patent No. CN201621237537.*